Journal of the Serbian Chemical Society

JSCS-info@shd.org.rs • www.shd.org.rs/JSCS

J. Serb. Chem. Soc. *78* (11) 1775–1787 (2013)
JSCS–4532

UDC 547.979.7+581.132:537.12+544.022
Original scientific paper

A study of the low-lying singlet and triplet electronic states of chlorophyll *a* and *b*

MIHAJLO ETINSKI*#, MILENA PETKOVIĆ# and MIROSLAV M. RISTIĆ#

Faculty of Physical Chemistry, University of Belgrade, Studentski trg 12–16, P. O. Box 47, 11158 Belgrade, Serbia

(Received 6 August, revised 23 September 2013)

Abstract: Chlorophylls have been extensively investigated both experimentally and theoretically owing to the fact that they are essential for photosynthesis. In the reported study, two forms of chlorophyll, chlorophyll *a* and chlorophyll *b*, were investigated by means of the density functional theory. Optimization of the S_0, S_1 and T_1 states was performed with the B3-LYP functional. The computed fluorescence lifetimes show good agreement with available experimental data. The electronic adiabatic energies of S_1 and T_1 states are 2.09/2.12 and 1.19/1.29 eV for chlorophyll *a* and chlorophyll *b*, respectively. The implications of these results on triplet formation are discussed. In addition, the calculated vertical ionization potentials showed good agreement with the experimental results.

Keywords: electronic states, density functional theory, photosynthesis.

INTRODUCTION

Chlorophylls are green photosynthetic pigments found in plants, algae and cyanobacteria. They play a vital role in photosynthesis, a process in which plants transform light into chemical energy.[1] They are arranged in and around pigment–protein complexes called photosystems, which are embedded in the thylakoid membranes of chloroplasts. Their function is twofold: to serve as collectors of photo-energy and as electron donors in reaction centers. The vast number of chlorophylls absorbs light and transfer that light energy by resonance energy transfer to a specific chlorophyll pair in the reaction center of photosystems. The excited state of the special pair of chlorophyll molecules is lower in energy than that for single chlorophyll molecules, allowing reaction centers to trap the energy transferred from other chlorophylls. The special pair undergoes a charge sepa-

* Corresponding author. E-mail: etinski@ffh.bg.ac.rs
# Serbian Chemical Society member.
doi: 10.2298/JSC130806096E

ration, a specific redox reaction in which the chlorophyll donates an electron into a series of molecular intermediates, called an electron transport chain.

The multipurpose role of chlorophylls is a consequence of their chemical structure, which is that of a macrocyclic π-electron system. They contain chlorin, a dihydrogen-reduced ring skeleton of porphyrin, with a magnesium atom in its center, Fig. 1. The ring carbon atoms are labeled from 1 to 20 according to IUPAC nomenclature. Attached to the chlorin are side chains. There are several types of chlorophyll depending on the side chains. In this work, the two most common chlorophylls, chlorophyll *a* (Chl *a*) and chlorophyll *b* (Chl *b*), will be considered. Both Chl *a* and *b* have a long insoluble carbon–hydrogen (phytyl) chain. In addition, Chl *a* contains only methyl groups as short side chains while in Chl *b*, a methyl group at the C3 position on the chlorin ring is replaced with an aldehyde group.

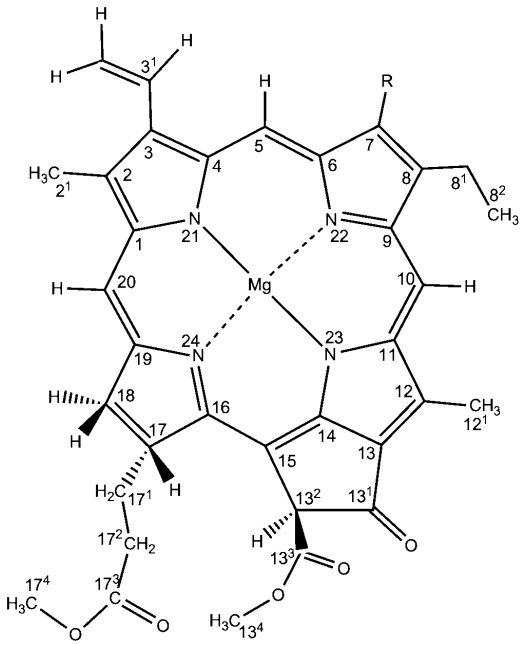

Fig. 1. The molecular structure and atom labels of Chl *a* (R=CH_3) and Chl *b* (R=COH).

Because of their fundamental significance to photosynthesis, the spectral and kinetic properties of Chl *a* and *b* have been studied extensively by both experimental[2–20] and theoretical[21–31] methods. The crystal structure of ethyl chlorophyllide *a* and *b*, chlorophylls that contain ethyl group instead of phytyl chain, was determined a long time ago.[4,18]

The electronic spectrum of chlorophylls is similar to that of a free-base porphyrin (FBP). The low-energy spectrum of FBP consists of two major absorption

bands: a weak Q band in visible region (500–650 nm) and intense (Soret) B band in the near-UV region (350–400 nm). FBP belongs to the D_{2h} point group and, therefore, each of these bands consists of two components polarized in the *x* and *y* directions. The Q and B bands are qualitatively understood by the Goutermann four-orbital model.[30] They stem from electron promotions involving the two highest occupied molecular orbitals (HOMOs) and two lowest unoccupied molecular orbitals (LUMOs). In the case of chlorophylls, due to the presence of side groups, the electronic transitions are not degenerated and are therefore split into distinct *x* and *y* polarized bands (Q_y, Q_x, B_y and B_x). In addition, the Q_y transition gains considerable intensity relative to those observed in porphyrins. Thomas *et al*.[3] measured the spectrum of Chl *a* in ACN–MeOH solution and found that the splitting was much greater between the Q_x and the Q_y transitions than between the B_x and B_y bands. In addition, they observed four peaks in the region of Q_x and the Q_y transitions belonging to 0–0 transitions and combinations of the 1–0 and 2–0 transitions. The lowest frequency band was conclusively assigned to the Q_y(0–0) transition but the precise location of the Q_x(0–0) transition remains unclear. The band positions in the spectrum of Chl *a* depend on the solvent and temperature.[5,11,19]

Shafizadeh *et al*.[5] used a supersonic cooled molecular beams to observe light absorption and ionization of isolated Chl *a*. They found that the Q_y band of Chl *a* was centered at 647 nm and the ionization potential was estimated to be 6.10±0.05 eV.

Kinetic studies showed that the lowest singlet excited state (S_1) of Chl *a* and its derivatives decay on several timescales. These decays include fluorescence, intersystem crossing (ISC) and internal conversion (IC). In all, the quantum yield of fluorescence was 0.32 and its lifetime was 6.0 ns[17]. The IC and ISC rates were determined to be 1.7×10^7 and 1.0×10^8 s^{-1}, respectively.[17] In a room temperature pyrimidine solution, the fluorescence and triplet lifetimes were 6.3 ns and 413±5 μs for Chl *a* and 3.2 ns and 556±62 μs for Chl *b*[14]. Interestingly, Renger and coworkers[6,8] found a thermally activated ISC in the Chl *b* homodimer but not in the Chl *a* homodimer.

The decay of the S_1 state of photochlorophyllide *a*, a precursor in the biosynthesis of chlorophyll *a*, occurred on the time scales of 4.27 and 200 ps.[9] Dietzek *et al*.[9] attributed these decay constants to solvent-induced vibrational cooling, formation of an intermediate state and its subsequent decay to the ground state, respectively.

Density functional theory[22,23,26–28,32,33] (DFT) has been the most frequently employed theoretical method to examine electronic states of chlorophylls, although the symmetry adapted cluster configuration interaction method,[31] semi-empirical[29] and multireference configuration interaction methods based on density functional theory[21] were used as well. This is due to the advantages of the

density functional over the other methods, which include features like calculation speed and reliability.

The main goal of this contribution was to gain some insight into the characters and geometries of the low-lying excited states of Chl *a* and *b*. In this respect, the geometries of the ground, the first excited singlet and the lowest triplet state were optimized. The similarities and differences between the electronic states of Chl *a* and *b* were also investigated.

In order to limit calculation to a manageable size, the phytyl ester in position 17 was replaced in all calculations with the methyl ester (Fig. 1). The obtained molecule is called methyl chlorophyllide. It was found that the replacement did not yield substantial change in any of the properties of chlorophyll. Therefore, the use of the abbreviations Chl *a* and *b* for methyl chlorophyllide *a* and *b* was retained.

COMPUTATIONAL DETAILS

All calculations were performed with the TURBOMOLE[34] program packages. We utilized DFT, unrestricted DFT (UDFT), and time-dependent DFT (TDDFT)[35] with the B3-LYP[36] functional implementation of TURBOMOLE for the ground-state and excited-state optimizations. It is known that the B3-LYP functional does not correctly describe charge transfer states that exist in chlorophylls.[22] This is due to the self-interaction error in the orbital energies obtained in the ground-state DFT calculation.[37] In this study, the transitions were limited to those that include only localized transitions.

All calculations were performed in C_1 point-group symmetry. SVP (Mg, 10s6p/4s2p; C, N, O, 7s4p1d/3s2p1d; H, 4s1p/2s1p) and TZVP (Mg, 14s7p/5s3p; C, N, O, 10s6p1d/4s3p1d; H, 5s1p/3s1p) basis sets from the TURBOMOLE was used. The structures of the ground and the lowest excited singlet, as well as the lowest triplet state were optimized using the SVP basis set. The vertical electronic excitation spectrum was calculated at B3-LYP/TZVP levels. This approach based on using a smaller basis set for geometry optimization and a larger for energy calculations previously gave good results.[38,39]

RESULTS AND DISCUSSION

The ground state geometry and vertical excitation spectrum

The bond lengths of the optimized ground state geometries of Chl *a* and *b* are presented in Table I together with data from crystallographic analysis.[4,18] For both molecules, the chlorin rings are planar with dihedral angles smaller than 2°. Nevertheless, the dihedral angle C18–C17–C16–N24 is approximately 14°. Moreover, in both molecules, the Mg atom is not centered in the middle of the chlorin ring but the N–Mg distances vary up to 0.160 Å. The N24–Mg bond is significantly longer than other N–Mg bonds. The average bond length difference between the optimized geometry and the crystallographic data for Chl *a* was 0.005 Å. The largest deviations were encountered for C2–C3 (0.037 Å), C12–C11 (0.036 Å), C13–$C13^1$ (0.034 Å), C18–$C18^1$ (0.035 Å) and O–$C17^4$ (0.042Å). Similarly, the average bond length difference for Chl *b* was 0.004 Å. The largest

deviations were found for C20–C1 (0.036 Å), C18–C18[1] (0.033 Å) and O–C17[4] (0.035Å). In both molecules, the longest C–C bond is C13[1]–C13[2]. The bond length differences between Chl *a* and *b* are smaller than 0.010 Å, except for the C7–C8, C8–C9 and C7–C7[1] bonds that are located near the aldehyde group of Chl *b*. It was concluded that the ground state geometries of Chl *a* and *b* are very similar. In addition, although the structures were optimized with a relatively small basis set, the bond lengths were similar to the experimental results.

TABLE I. Optimized S_0, S_1 and T_1 state bond lengths of Chl *a* and *b* in Å. Experimental bond lengths are crystallographic data from the literature[4,18]

Bond	Chl *a*				Chl *b*			
	S_0	S_0 (Exp.)	S_1	T_1	S_0	S_0 (Exp.)	S_1	T_1
C1–C2	1.454	1.451	1.443	1.442	1.457	1.456	1.442	1.441
C2–C3	1.384	1.347	1.394	1.397	1.383	1.353	1.395	1.399
C3–C4	1.467	1.476	1.468	1.454	1.471	1.453	1.470	1.454
C4–N21	1.379	1.384	1.370	1.360	1.382	1.402	1.372	1.359
C4–C5	1.394	1.370	1.413	1.443	1.389	1.384	1.408	1.444
C5–C6	1.415	1.419	1.403	1.376	1.421	1.415	1.406	1.378
C6–N22	1.362	1.361	1.372	1.390	1.356	1.359	1.368	1.389
C6–C7	1.454	1.464	1.464	1.472	1.454	1.439	1.462	1.468
C7–C8	1.381	1.362	1.376	1.367	1.397	1.370	1.391	1.381
C8–C9	1.456	1.463	1.465	1.478	1.443	1.438	1.454	1.469
C9–N22	1.376	1.388	1.372	1.357	1.382	1.399	1.376	1.359
C9–C10	1.408	1.378	1.413	1.415	1.412	1.392	1.416	1.418
C10–C11	1.401	1.415	1.405	1.404	1.396	1.397	1.402	1.401
C11–N23	1.391	1.402	1.390	1.393	1.394	1.406	1.390	1.396
N23–C14	1.334	1.347	1.338	1.335	1.332	1.335	1.339	1.334
C14–C13	1.424	1.416	1.427	1.417	1.425	1.420	1.426	1.417
C13–C12	1.393	1.405	1.394	1.403	1.390	1.372	1.392	1.409
C12–C11	1.456	1.420	1.461	1.457	1.458	1.439	1.463	1.456
C13–C13[1]	1.465	1.431	1.462	1.459	1.466	1.447	1.463	1.460
C13[1]–C13[2]	1.581	1.569	1.581	1.583	1.580	1.570	1.581	1.581
C13[2]–C15	1.536	1.535	1.533	1.534	1.536	1.531	1.532	1.534
C15–C14	1.418	1.398	1.418	1.437	1.418	1.418	1.417	1.439
C15–C16	1.385	1.365	1.389	1.367	1.384	1.393	1.382	1.366
C17–C18	1.550	1.556	1.549	1.548	1.549	1.566	1.549	1.548
C18–C19	1.525	–	1.522	1.523	1.525	1.532	1.522	1.523
C19–C20	1.393	1.384	1.396	1.406	1.393	1.411	1.394	1.407
C20–C1	1.413	1.389	1.416	1.409	1.413	1.377	1.418	1.409
C19–N24	1.356	1.348	1.364	1.347	1.356	1.328	1.366	1.346
N21–Mg	2.036	2.063	2.039	2.047	2.033	2.055	2.037	2.045
N22–Mg	2.077	2.094	2.073	2.073	2.085	2.102	2.081	2.086
N23–Mg	2.020	2.021	2.023	2.026	2.022	2.005	2.026	2.027
N24–Mg	2.159	2.167	2.150	2.140	2.156	2.165	2.154	2.140
C3–C3[1]	1.464	1.476	1.457	1.461	1.463	1.440	1.456	1.461
C3[1]–C3[2]	1.344	1.275	1.348	1.346	1.344	1.317	1.349	1.346

TABLE I. Continued

Bond	Chl *a*				Chl *b*			
	S_0	S_0 (Exp.)	S_1	T_1	S_0	S_0 (Exp.)	S_1	T_1
C2–C2[1]	1.498	1.496	1.498	1.497	1.498	1.508	1.498	1.498
C18–C18[1]	1.538	1.503	1.540	1.539	1.538	1.505	1.540	1.539
C1–N21	1.360	1.377	1.374	1.380	1.358	1.363	1.373	1.382
C16–N24	1.377	1.387	1.380	1.405	1.377	1.364	1.376	1.406
C7–C7[1]	1.499	1.501	1.497	1.497	1.462	1.460	1.461	1.466
C7[1]=O	–	–	–	–	1.218	1.233	1.219	1.216
C8–C8[1]	1.504	1.479	1.503	1.503	1.504	1.498	1.502	1.502
C8[1]–C8[2]	1.539	1.494	1.539	1.539	1.540	1.541	1.540	1.540
C12–C12[1]	1.496	1.490	1.494	1.494	1.496	1.477	1.493	1.494
C13[1]–O	1.211	1.233	1.214	1.214	1.211	1.235	1.213	1.213
C13[2]–C13[3]	1.523	1.501	1.523	1.522	1.524	1.538	1.524	1.523
C13[3]=O	1.208	1.184	1.208	1.208	1.208	1.189	1.208	1.208
C13[3]–O	1.343	1.337	1.343	1.343	1.342	1.339	1.342	1.342
O–C13[4]	1.428	1.443	1.428	1.427	1.428	1.410	1.429	1.428
C16–C17	1.525	1.524	1.520	1.521	1.523	1.531	1.520	1.521
C17–C17[1]	1.546	1.534	1.549	1.547	1.547	1.520	1.549	1.548
C17[1]–C17[2]	1.529	1.536	1.528	1.528	1.528	1.539	1.528	1.528
C17[2]–C17[3]	1.515	1.495	1.516	1.516	1.516	1.478	1.516	1.516
C17[3]=O	1.207	1.213	1.207	1.207	1.207	1.216	1.206	1.206
C17[3]–O	1.348	1.339	1.347	1.348	1.348	1.336	1.347	1.347
O–C17[4]	1.428	1.470	1.428	1.428	1.428	1.463	1.428	1.428

The frontier Kohn–Sham orbitals are presented in Fig. 2. The depicted orbitals have the same structure for both molecules. Generally, the occupied Chl *b* orbitals have lower energies than the Chl *a* orbitals, and the opposite is true for the unoccupied orbitals. All presented orbitals are π orbitals. The oxygen *n* orbitals are lower in energy. The HOMO-1, HOMO, LUMO and LUMO+1 electron densities are located on the chlorin ring.

In Tables II and III, the calculated first two singlet and four triplet excitation energies and oscillator strengths of Chl *a* are compared with those of other methods and experimental data. By comparing SVP and TZVP results, generally, it was found that triple zeta basis lowers the excitation energies by at most 0.05 eV. In addition, no effect on the excitation energies was found upon adding a phytyl tail to methyl chlorophylide.

The singlet excited states are Q_y and Q_x in accordance with other methods and experimental results. The oscillator strength of the Q_y state is larger by an order of magnitude than that of the Q_x state. Their energies are similar to experimental results, with respect that Q_x is better described with the B3-LYP/CAM--B3LYP functional.

The triplet states have different electronic structures compared with those of the singlet states. The lowest triplet state comes predominantly from HOMO to

LUMO transition. Its energy is 0.8 eV lower than that of the S_1 state, according to the B3-LYP results. There are three triplet states below the S_1 state. The $T_2/T_3/T_4$ states come primarily from HOMO-1 to LUMO/HOMO to LUMO+1/ /HOMO-1 to LUMO+1 excitation.

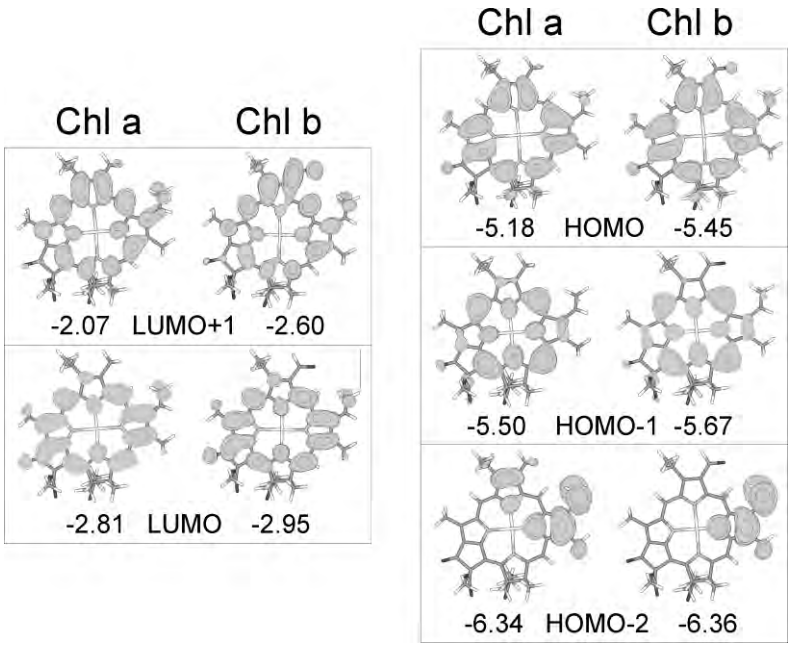

Fig. 2. Selected B3-LYP/TZVP frontier molecular orbitals and their energies.

TABLE II. Vertical excitation spectrum of the ground state of Chl *a*. All energies are in eV. Oscillator strengths are given in parentheses

State	Excitation	TDDFT/ B3-LYP/ /TZVP, this work	TDDFT/ B-P/ /SV(P)[23]	TDDFT/ /CAM- -B3LYP/ 6-31G*[22]	SAC-CI/ 6-31G*[22]	DFT/MRCI /BH-LYP/ VDZP[21]	Exp.
S_1	HOMO→LUMO (85.0 %), HOMO-1→ →LUMO+1 (14.5 %)	2.11 (0.2207)	2.00 (0.1820)	2.10 (0.2400)	1.75 (0.2900)	2.01 (0.4573)	1.87,[3] 1.88,[15] 1.86,[2] 1.92[5]
S_2	HOMO-1→LUMO (70.0 %), HOMO→LUMO+1 (28.3 %)	2.28 (0.0247)	2.04 (0.0260)	2.47 (0.0260)	2.26 (0.0180)	2.27 (0.0444)	2.14,[3] 2.16[15]
T_1	HOMO→LUMO (93.5 %)	1.32	–	–	–	–	–
T_2	HOMO-1→LUMO (88.9 %)	1.54	–	–	–	–	–
T_3	HOMO→LUMO+1 (90.8 %)	2.04	–	–	–	–	–
T_4	HOMO-1→ →LUMO+1 (85.2 %)	2.35	–	–	–	–	–

TABLE III. Vertical excitation spectrum of the ground state of Chl *b*. All energies are in eV. Oscillator strengths are given in parentheses

State	TDDFT/B3-LYP/ TPZV	Exp.
S_1	**2.14** (0.1303)	1.92 (in toluene[2])
	HOMO→LUMO (74.9 %), HOMO-1→LUMO+1 (22.1 %)	
S_2	**2.25** (0.0006)	–
	HOMO-1→LUMO (56.7 %), HOMO→LUMO+1 (40.5 %)	
T_1	**1.44**	–
	HOMO→LUMO (86.9 %)	
T_2	**1.58**	–
	HOMO-1→LUMO (86.4 %)	
T_3	**1.84**	–
	HOMO→LUMO+1 (91.4 %)	
T_4	**2.10**	–
	HOMO-1→LUMO+1 (86.9 %)	

Chl *b* has similar electronic states to those of Chl *a*, but there are some minor differences. Its excited state energies and oscillator strengths are given in Table IV. The first two singlet excited states are Q_y and Q_x. They have energies that are very similar to those of Chl *a*.

TABLE IV. Vertical excitation spectrum of the S_1 state of Chl *a* and *b*. All energies are in eV. Oscillator strengths are given in parentheses

State	Chl a	Chl b
S_0	**0.05**	**0.06**
S_1	**2.09** (0.2377)	**2.12** (0.1555)
	HOMO→LUMO (86.7 %)	HOMO→LUMO (78.9 %)
S_2	**2.30** (0.0290)	**2.25** (0.0002)
	HOMO-1→LUMO (69.7 %),	HOMO-1→LUMO (55.2 %),
	HOMO→LUMO+1 (28.2 %)	HOMO→LUMO+1 (42.3 %)
T_1	**1.28**	**1.39**
	HOMO→LUMO (94.7 %)	HOMO→LUMO (90.6 %)
T_2	**1.53**	**1.56**
	HOMO-1→LUMO (89.2 %)	HOMO-1→LUMO (86.0 %)
T_3	**2.05**	**1.84**
	HOMO→LUMO+1 (88.7 %)	HOMO→LUMO+1 (88.4 %)
T_4	**2.34**	**2.13**
	HOMO-2→LUMO (70.0 %)	HOMO-1→LUMO+1 (70.2 %)

The triplet states of Chl *b* have the same ordering and basically the same structure as those of Chl *a*. The T_1 state is 0.7 eV lower than the S_1 state. Moreover, B3-LYP predicts four triplet states below the S_1 state, one more than in Chl *a*. This finding is in line with the work of Renger and coworkers[6] on thermally activated ISC in chlorophylls. They proposed that the additional triplet state that is below the S_1 state in Chl *b* is responsible for the thermally activated

ISC. The present calculation showed that it is 0.04 eV lower than the S_1 state. In Chl *a*, the T_4 state is 0.24 eV higher than the S_1 state and it is not thermally accessible ($kT \approx 0.03$ eV). Hence, a small difference in the structure of chlorophyll can significantly change the photophysical properties.

The S_1 state geometry and vertical excitation spectrum

The optimized S_1 state is the Q_y state for Chl *a* and *b*. The optimized bond lengths are presented in Table I. The S_1 state comes from HOMO to LUMO excitation so the change of electronic density is located on the chlorin ring. The largest changes are in the C–C bonds. For Chl *a*, C4–N21 (0.009 Å), C4–C5 (0.019 Å), C8–C9 (0.009 Å) bonds elongate while C1–C2 (0.011 Å) and C5–C6 (0.012 Å) bonds shrink. Similarly, for Chl *b*, the largest changes are for C1–C2 (–0.015 Å), C4–C5 (+0.019 Å) and C5–C6 (–0.015 Å) bonds. The bond length changes are rather small indicating a small geometry displacement upon excitation. This can be seen as well from the adiabatic energy that is 2.09 and 2.12 eV for Chl *a* and *b*, respectively, as predicted by B3-LYP. Hence, the optimization stabilizes the S_1 state by 0.02 eV, confirming that its geometry is close to the ground state geometry. The general spectroscopic consequence of this small geometry change is that the 0–0 transition should be pronounced in absorption spectrum if the Franck–Condon approximation were valid. However, in chlorophylls, the Franck–Condon approximation is not sufficient due to the small transition dipole moment at the equilibrium geometry of the ground state and hence the 0–0 transition is not dominant.

The vertical singlet and triplet excitation energies for Chl *a* and *b* are given in Table V. The order and character of the excited singlet states of Chl *a* remain the same as at the ground state geometry. A similar situation was found for the triplet states, with the exception of the fourth state. This state comes predominantly from HOMO-2 to LUMO excitation starting from the S_1 optimized geometry and from HOMO-1 to LUMO+1 transition from the true ground state.

The fluorescence lifetimes were calculated using the oscillator strength and excitation energies. Chl *a* has a larger oscillator strength than Chl *b* and therefore, its fluorescence lifetime is larger as well. The calculated values are 7.3 and 10.8 ns. The value for Chl *a* is close to experimentally determined values of 6.0 and 6.2 ns in ether[17] and toluene,[2] respectively. The ISC decay rate is of the order of 10 ns for Chl *a*, making the radiative and non-radiative processes competitive.

The T_1 state and vertical excitation spectrum

The lowest triplet state comes from HOMO to LUMO excitation. Its optimized bond lengths are presented in Table I. The largest differences with respect to the ground state geometry are for the C4–C5, C5–C6, C6–N22 and C16–N24

bonds. The adiabatic energies of T_1 state are 1.19 and 1.29 eV for Chl *a* and *b*, respectively. The T_1 state energies are lower by 0.13 and 0.15 eV than at the ground state geometry.

TABLE V. Vertical excitation spectrum of the T_1 state of Chl *a* and *b*. All energies are in eV. Oscillator strengths are given in parentheses

State	Chl a	Chl b
S_0	**0.15**	**0.18**
S_1	**2.14** (0.2641) HOMO→LUMO (89.5 %)	**2.19** (0.2050) HOMO→LUMO (85.1 %)
S_2	**2.41** (0.0357) HOMO-1→LUMO (68.9 %), HOMO→LUMO+1 (28.9 %)	**2.36** (0.0001) HOMO-1→LUMO (50.6 %), HOMO→LUMO+1 (45.9 %)
T_1	**1.19** HOMO→LUMO (95.4 %)	**1.29** HOMO→LUMO (94.1 %)
T_2	**1.68** HOMO-1→LUMO (90.4 %)	**1.72** HOMO-1→LUMO (84.2 %)
T_3	**2.19** HOMO→LUMO+1 (90.1 %)	**1.96** HOMO→LUMO+1 (86.7 %)
T_4	**2.41** HOMO-2→LUMO (80.1 %)	**2.28** HOMO-2→LUMO (70.9 %)

The vertical singlet and triplet excitation energies at T_1 geometry are given in Table V. At this geometry, the singlet states have slightly smaller energies than at the S_1 geometry.

The S_1–T_1 adiabatic energy gap is 0.90 and 0.83 eV for Chl *a* and Chl *b*, respectively. The lower value for Chl *b* has an implication on the ISC transition from S_1 to T_1 state. The energy gap law[40,41] states that for electronic states with similar geometries, the smaller the energy gap, the larger is the ISC rate. Hence, in the case of Chl *a* and *b*, assuming the same spin-orbit matrix elements and geometries of the S_1 and T_1 electronic states, Chl *b* will have a faster ISC rate for triplet formation.

The ionization potential

Chlorophylls play an important role in the initial electron transfer step in photosynthesis. Thus, an estimation of their ionization potential is necessary in order to understand the electron transfer process. Recently, Shafizadeh *et al*.[5] measured the ionization potential (IP) of Chl *a* in a supersonic beam using a one color two photon experiment. They reported a value 6.10±0.05 eV.

In order to obtain the vertical IP for Chl *a* and *b*, an unrestricted DFT calculation was performed on the cationic state at the respective ground state geometries. The IPs were determined to be 6.19 and 6.45 eV with the SVP basis set and 6.28 and 6.54 eV with the TZVP basis set for Chl *a* and Chl *b*, respectively. The increase of the IP with the basis set is a consequence of the greater

stabilization of the cationic state with respect to the ground state. It was expected that Chl *b* would have a higher IP than Chl *a* because, according to a simple rule,[42] the IP value is proportional to the negative energy of the HOMO orbital. The implication of this result is that it is easier to ionize Chl *a* than Chl *b*.

A preliminary calculation with the SVP basis set showed that the IP of the full form of Chl *a* is 6.16 eV. This means that the phytyl tail had almost no influence on the IP. Hasegawa and Noguchi[43] using a much bigger basis set 6-311+G(d) obtained an IP of 6.23 eV.

CONCLUSIONS

Density functional theory and its time dependent variant were employed for an investigation of the structure and electron excitation to the four lowest singlet and triplet states of chlorophyll *a* and *b*. It was determined that the phytyl group did not significantly influence the electron spectra of the two investigated systems. Thus, the methyl ester was used instead of the phatyl ester in order to decrease the computational effort. The two structures optimized at the B3-LYP/ /SVP level show good agreement with the available experimental data, even though a modest basis set was employed. Optimization of the lowest excited singlet and triplet states did not change the structures significantly. The electronic adiabatic energies of the S_1 and T_1 states are 2.09/2.12 and 1.19/1.29 eV for Chl *a* and Chl *b*, respectively.

Vertical excitation energies and estimated fluorescence lifetimes were comparable with experimental literature values. Difference in positions of the energy levels in Chl *a* and Chl *b* explained the experimental finding that thermally activated intersystem crossing occurs in Chl *b*, and that Chl *b* has a larger intersystem crossing rate. On the other hand, the larger oscillator strength in Chl *a* explains its longer fluorescence lifetime. The computed ionization potentials were in good agreement with the previously reported measured values, and they imply easier ionization of Chl *a* compared to Chl *b*.

The obtained results confirmed that DFT and TD–DFT calculations could provide useful information about structure and electron transitions (electron spectra, excited state dynamics and ionization) in large systems, such as chlorophyll, and were able to explain the different behavior of different types of chlorophylls.

Acknowledgement. The authors acknowledge the Ministry of Education, Science and Technological Development of the Republic of Serbia for the financial support (Contract No. 172040).

И З В О Д

ПРОУЧАВАЊЕ СИНГЛЕТНИХ И ТРИПЛЕТНИХ ЕЛЕКТРОНСКИХ СТАЊА ХЛОРОФИЛА *a* И *b*

МИХАЈЛО ЕТИНСКИ, МИЛЕНА ПЕТКОВИЋ и МИРОСЛАВ М. РИСТИЋ

Факултет за физичку хемију, Универзитет у Београду, Студентски Трг 12–16, 11158 Београд

Због огромног значаја за фотосинтезу хлорофили су доста проучавани експериментално и теоријски. Ми смо помоћу теорије функционала густине проучавали два облика хлорофила, хлорофил *a* и холорофил *b*. Опмизација S_0, S_1 и T_1 стања је извршена помоћу B3-LYP функционала. Израчуната времена флуоросценције се добро слажу са доступним експерименталним подацима. Електронске адијабатске енергије S_1 и T_1 стања су 2,09/2,12 и 1,19/1,29 eV за хлорофил *a* и хлорофил *b*. Продискутоване су последице ових резултатат на стварање триплетног стања. Такође, израчунати вертикални јонизациони потенцијали се добро слажу са експерименталним резултатима.

(Примљено 6. августа, ревидирано 23. септембра 2013)

REFERENCES

1. J. M. Berg, L. J. Tymoczko, L. Stryer, *Biochemistry,* 5th ed., W. H. Freeman, New York, USA, 2002
2. J. W. Springer, K. M. Faries, J. R. Diers, C. Muthiah, O. Mass, H. L. Kee, C. Kirmaier, J. S. Lindsey, D. F. Bocian, D. Holten, *Photochem. Photobiol.* **88** (2012) 651
3. L. L. Thomas, J. H. Kim, T. M. Cotton, *J. Am. Chem. Soc.***112** (1990) 9378
4. H. Chow, R. Serlin, C. E. Strouse, *J. Am. Chem. Soc.* **97** (1975) 1230
5. N. Shafizadeh, M. H. Ha-Thi, B. Soep, M. Gaveau, F. Piuzzi, C. Pothier, *J. Chem. Phys.* **135** (2011) 114303
6. T. Renger, M. E. Madjet, F. Müh, I. Trostmann, F.-J. Schmitt, C. Theiss, H. Paulsen, H. J. Eichler, A. Knorr, G. Renger, *J. Phys. Chem., B* **113** (2009) 9948
7. R. S. Knox, J. S. Brown, P. D. Laible, M. F. J. Talbot *Photosynth. Res.* **60** (1999) 165
8. F.-J. Schmitt, I. Trostmann, C. Theiss, J. Pieper, T. Renger, J. Fuesers, E. H. Hubrich, H. Paulsen, H. J. Eichler, G. Renger, *J. Phys. Chem., B* **112** (2008) 13951
9. B. Dietzek, R. Maksimenka, T. Siebert, E. Birckner, W. Kiefer, J. Popp, G. Hermann, M. Schmitt, *Chem. Phys. Lett.* **397** (2004) 110
10. Y. Shiu, *Chem. Phys. Lett.* **378** (2003) 202.
11. B. Mysliwa-Kurdziel, J. Kruk, K. Strzalka, *Photochem. Photobiol.* **79** (2004) 62
12. T. Noguchi, T. Tomo, C. Kato, *Biochemistry* **40** (2001) 2176
13. R. Hanf, S. Tschierlei, B. Dietzek, S. Seidel, G. Hermann, M. Schmitt, J. Popp, *J. Raman Spectrosc.* **41** (2010) 414
14. D. M. Niedzwiedzki, R. E. Blankenship, *Photosynth. Res.* **106** (2010) 227
15. C. Houssier, K. Sauer, *J. Am. Chem. Soc.* **92** (1970) 779
16. Y. Shi, J.-Y. Liu, K.-L. Han, *Chem. Phys. Lett.* **410** (2005) 260
17. D. Leupold, A. Struck, H. Stiel, K. Teuchner, S. Oberlaender, H. Scheer, *Chem. Phys. Lett.* **170** (1990) 478.
18. R. Serlin, H.-C. Chow, C. E. Strouse, *J. Am. Chem. Soc.* **97** (1975) 7237
19. L. Fiedor, M. M. Stasiek, B. Myśliwa-Kurdziel, K. Strzałka, *Photosynth. Res.* **78** (2003) 47
20. M. Rätsep, J. Linnanto, A. Freiberg, *J. Chem. Phys.* **130** (2009) 194501
21. A. B. J. Parusel, S. Grimme, *J. Phys. Chem., B* **104** (2000) 5395

22. Z.-L. Cai, M. J. Crossley, J. R. Reimers, R. Kobayashi, R. D. Amos, *J. Phys. Chem., B* **110** (2006) 15624
23. D. Sundholm, *Chem. Phys. Lett.* **302** (1999) 480
24. K. Karki, D. Roccatano, *J. Chem. Theory. Comput.* **7** (2011) 1131
25. A. Pandey, S. N. Datta, *J. Phys. Chem., B* **109** (2005) 9066
26. S. Parameswaran, R. Wang, G. Hastings, *J. Phys. Chem., B* **112** (2008) 14056
27. S. Sinnecker, W. Koch, W. Lubitz, *J. Phys. Chem., B* **106** (2002) 5281
28. R. Wang, S. Parameswaran, G. Hastings, *Vib. Spectrosc.* **44** (2007) 357
29. J. Linnanto, J. Korppi-Tommola, *Phys. Chem. Chem. Phys.* **2** (2000) 4962
30. M. Gouterman, *J. Mol. Spectrosc.* **6** (1961) 1139
31. J. Hasegawa, Y. Ozeki, K. Ohkawa, M. Hada, H. Nakatsuji, *J. Phys. Chem., B* **102** (1998) 1320
32. A. Marchanka, W. Lubitz, M. Van Gastel, *J. Phys. Chem., B* **113** (2009) 6917
33. D. Kröner, J. P. Götze, *J. Photochem. Photobiol., B* **109** (2012) 12.
34. Turbomole V6.4 2012, University of Karlsruhe and Forschungszentrum Karlsruhe GmbH., 1989–2007, TURBOMOLE GmbH, since 2007 available from www.turbomole.com
35. R. Bauernschmitt , R. Ahlrichs, *Chem. Phys. Lett.* **256** (1996) 454.
36. A. D. Becke, *J. Chem. Phys.* **98** (1993) 5648.
37. A. Dreuw, M. Head-Gordon, *J. Am. Chem. Soc.* **126** (2004) 4007
38. M. Etinski, T. Fleig, C. M. Marian, *J. Phys. Chem., A* **113** (2009) 11809
39. L. Pohler, M. Kleinschmidt, M. Etinski, C. M. Marian, *Mol. Phys.* **110** (2012) 2429
40. R. Englman, J. Jortner, *Mol. Phys.* **18** (1970) 145
41. M. Etinski, C. M. Marian, *Phys. Chem. Chem. Phys.* **12** (2010) 15665
42. C.-G. Zhan, J. A. Nichols, D. A. Dixon, *J. Phys. Chem., A* **107** (2003) 4184
43. K. Hasegawa, T. Noguchi, Biochemistry **44** (2005) 8865.